Journal of Power Sources 220 (2012) 65–73

Contents lists available at SciVerse ScienceDirect

Journal of Power Sources

journal homepage: www.elsevier.com/locate/jpowsour

A comparative study of ORR at the Pt electrode in ammonium ion-contaminated H_2SO_4 and $HClO_4$ solutions

Mohammad R. Rahman [a,b], Mohamed I. Awad [a,c], Fusao Kitamura [a], Takeyoshi Okajima [a], Takeo Ohsaka [a,*]

[a] Department of Electronic Chemistry, Interdisciplinary Graduate School of Science and Engineering, Tokyo Institute of Technology, 4259-G1-5, Nagatsuta, Midori-ku, Yokohama 226-8502, Japan
[b] 506-300 Mary St. N., Oshawa, ON L1G 5C8, Canada
[c] Department of Chemistry, Faculty of Science, Cairo University, Cairo, Egypt

HIGHLIGHTS

► Poisoning of the Pt electrode by low concentration NH_4^+ ion was investigated in H_2SO_4 and $HClO_4$ solutions.
► Significant poisoning was observed in H_2SO_4 solution.
► An extraordinary recovery of the poisoned electrode was achieved in $HClO_4$ solution.
► The Tafel slopes were affected by NH_4^+ ion in H_2SO_4 but not in $HClO_4$ solution.

ARTICLE INFO

Article history:
Received 30 March 2012
Received in revised form
21 June 2012
Accepted 31 July 2012
Available online 8 August 2012

Keywords:
Poisoning
Oxygen reduction
Recovery
Ammonium ion

ABSTRACT

Poisoning of the poly-Pt electrode by low concentration ammonium ion was investigated in H_2SO_4 and $HClO_4$ solutions and a significant poisoning was observed in H_2SO_4 solution. An extraordinary recovery of the poisoned electrode was achieved in $HClO_4$ solution by cycling the electrode potential between the onset potentials of the hydrogen and oxygen evolution. The extent of recovery was marked using the oxygen reduction reaction (ORR) as a probing reaction. Ammonium ion poisoning of the electrodes in H_2SO_4 caused a significant contribution of the two-electron reduction of O_2 to hydrogen peroxide, as indicated by the rotating ring-disk voltammetry. The Tafel slopes at the low and high current densities were also affected by the presence of ammonium ion in H_2SO_4 solution and an increase in the Tafel slope was recognized with increasing the concentration of ammonium ion. However, the Tafel slopes at the low and high current densities were hardly affected by the ammonium ion in $HClO_4$ solution.

1. Introduction

In recent years, proton exchange membrane fuel cells (PEMFCs), in which electrochemical oxygen reduction reaction (ORR) is the prime reaction, have become a subject of considerable interest because it may add promising advances in the energy conversion technology [1–7]. During fuel cell operation, polarization at the cathode (oxygen reduction) is highly significant compared to that at the anode and thus much efforts have been devoted to the study of the factors affecting the cathodic reaction including the adsorption of several poisoning species. Common air-borne poisons (e.g., sulphur dioxide (SO_2), nitrogen dioxide (NO_2)), and other contaminants (e.g., ammonium (NH_4^+) ion) have deleterious effects on PEMFC performance [8–13]. The poisoning effect of the adsorbed SO_2 on the polycrystalline platinum (poly-Pt) electrode has been studied extensively [11,14–24]. However, a little attention has been paid to the poisoning effect of NH_4^+ ion on the poly-Pt electrode towards ORR [25,26]. Although various studies have demonstrated that NH_4^+ ion has a negative effect on PEMFC performance, especially the major poisoning effect of NH_4^+ ion at the anode [27,28], studies of phosphoric acid FCs have revealed that there is a significant effect of NH_4^+ ion on the ORR [29].

The aim of the present work is to explore the effects of the low concentration NH_4^+ ion poisoning on the ORR at the poly-Pt electrodes in sulphuric (H_2SO_4) and perchloric ($HClO_4$) acid solutions at ambient temperature (25 °C). H_2SO_4 and $HClO_4$ are often used as electrolyte solutions in the electrochemical studies for developing PEMFCs, especially the fundamental electrocatalysis of their electrocatalysts, while in PEMFCs Nafion® is typically used as polymer

* Corresponding author. Tel.: +81 45 924 5404; fax: +81 45 924 5489.
E-mail address: ohsaka@echem.titech.ac.jp (T. Ohsaka).

0378-7753/$ – see front matter © 2012 Elsevier B.V. All rights reserved.
http://dx.doi.org/10.1016/j.jpowsour.2012.07.103

electrolyte membrane. It is noteworthy to mention here that $HClO_4$ solution is usually used for the study of the electrochemical behaviour of ORR because the perchlorate is nonadsorbable anion, similar to the solid acid (Nafion®), while the adsorption of bisulphate and sulphate anions is evident on the Pt surface [30,31]. Recovery of the poisoned electrodes is examined by cycling the electrode potential (starting from the open circuit potential towards either cathodic or anodic direction of potential) between 0.06 and 1.56 V vs. RHE for 10 cycles at 100 mV s^{-1} in NH_4^+ ion-free H_2SO_4 or $HClO_4$ solutions. In addition, the effect of the adsorbed NH_4^+ on the mechanism of the ORR is elucidated using rotating ring-disk electrode (RRDE) methodology [32,33]. The rotating disk measurements permit a correction for diffusion limitations of the oxygen gas (O_2) in solution at high potentials, allowing isolation of the ORR kinetics. The additional ring, which surrounds the central disk with the electrocatalyst, is used to oxidize any hydrogen peroxide (H_2O_2) that forms at the disk-electrocatalyst. With this approach, we can resolve whether a trace of adsorbed NH_4^+ ion changes the mechanism of the oxygen reduction from four-electron pathway to two-electron pathway forming H_2O_2 or not. Similar experiments have also been performed at the pre-oxidized and pre-reduced poly-Pt electrodes in the presence of various concentrations of NH_4^+ ion. Although the present cases are not exactly the real one, the comparative study may help to provide better understanding of NH_4^+ ion-poisoning effects and recovery approaches that may be used in the recovery of PEMFC performance.

2. Experimental

All the electrochemical measurements were performed and recorded using a computer-controlled ALS CHI-760D electrochemical analyser, driven with a general-purpose electrochemical system software (BAS). Steady-state voltammograms were obtained at the RRDE using a rotary system from Nikko Keisoku, Japan. A conventional three-electrode cell of around 20 cm^3 was used for the cyclic voltammetric measurements, while in the case of hydrodynamic voltammetric measurements the working electrode compartment was 200 cm^3 to eliminate any possible changes in the O_2 concentration during the measurements. Poly-Pt electrode of 1.6 mm in diameter was employed for the cyclic voltammetric measurements while steady-state voltammograms were measured using the RRDE with Pt-disk (6.0 mm in diameter) and Pt-ring. A spiral Pt wire and an Ag|AgCl|KCl (sat.) were used as counter and reference electrodes, respectively. All the potential values in the text and figures are mentioned with respect to a reversible hydrogen electrode (RHE). Prior to use, the poly-Pt electrode was polished first with no. 2000 emery paper, then with aqueous slurries of successively finer alumina powder (particle size down to 0.06 mm) with the help of a polishing microcloth. The electrode was then sonicated for 10 min in milli-Q water followed by potential cycling between the onset potentials of the hydrogen and oxygen evolution until the voltammetric characteristic of clean Pt electrode was obtained. The Pt disk–Pt ring RRDE was cleaned in the same manner as the poly-Pt electrode. The potential of the Pt-disk was held for 10 min at 1.06 V or 0.06 V vs. RHE to obtain pre-oxidized or pre-reduced electrodes, respectively. No such pre-treatment was performed for the Pt-ring electrode.

NH_4^+ ion-poisoned solution was prepared by introducing a specific volume of 30% NH_3 solution in either 0.1 M H_2SO_4 or 0.1 M $HClO_4$ solution giving a desired concentration of the NH_4^+ ion. Prior to each experiment, either N_2 or O_2 gas was bubbled directly into the cell for 30 min to obtain either N_2 or O_2 saturated solution and electrochemical measurements were carried out under either of these two gases according to the requirement. All the measurements were accomplished at room temperature (25 ± 1 °C). All of the reagents (of analytical grade) used in this study were purchased from either Kanto Chemicals Co. Ltd. (Tokyo, Japan) or Wako Pure Chemicals Industries Ltd. (Osaka, Japan) and used without further purification. All the solutions were prepared with Milli-Q (18 MΩ cm) deionized water.

3. Results and discussion

The characteristic current–potential (I–E) curves at the poly-Pt electrode in deoxygenated (i.e., N_2-saturated) 0.1 M H_2SO_4 and 0.1 M $HClO_4$ solutions are shown in Fig. 1(A) and (B), respectively (black lines). In the presence of 1 ppm NH_4^+ ion, in the anodic potential scan, the charge for the hydrogen desorption peaks was noticed to be decreased in both electrolytic media. It decreased further with increasing the concentration of NH_4^+ ion. The Pt oxide layer formation region was also affected. The current of the onset of the oxide layer formation (at 0.86 V vs. RHE) was found to decrease with increasing the NH_4^+ ion concentration. There was also a slightly higher oxidation current at potentials above 1.16 V vs. RHE

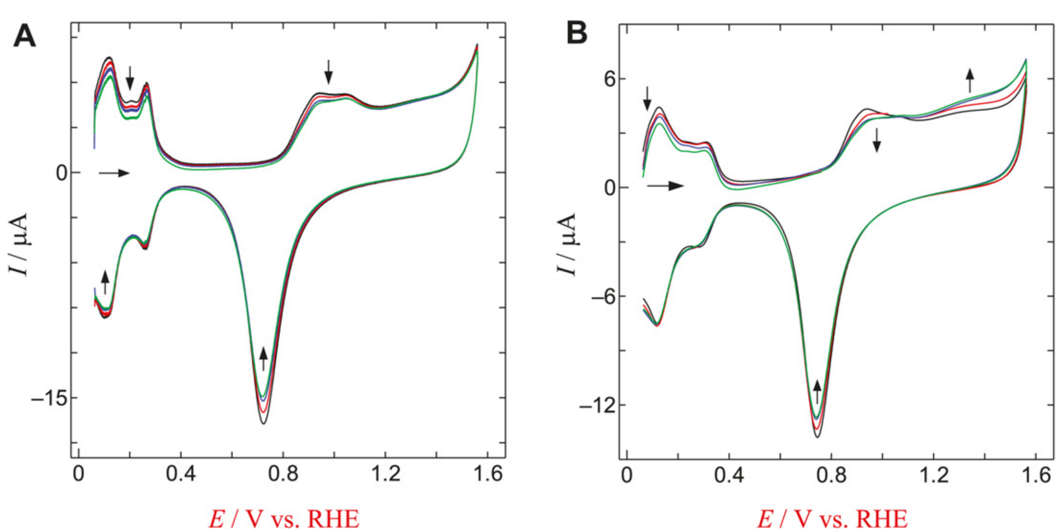

Fig. 1. CVs obtained at the poly-Pt electrode in N_2-saturated 0.1 M H_2SO_4 (A) and 0.1 M $HClO_4$ (B) solutions containing 0 (Black), 1 (Red), 10 (Blue) and 100 (Green) ppm NH_4^+ ion. Scan rate: 100 mV s^{-1}. (For interpretation of the references to colour in this figure legend, the reader is referred to the web version of this article.)

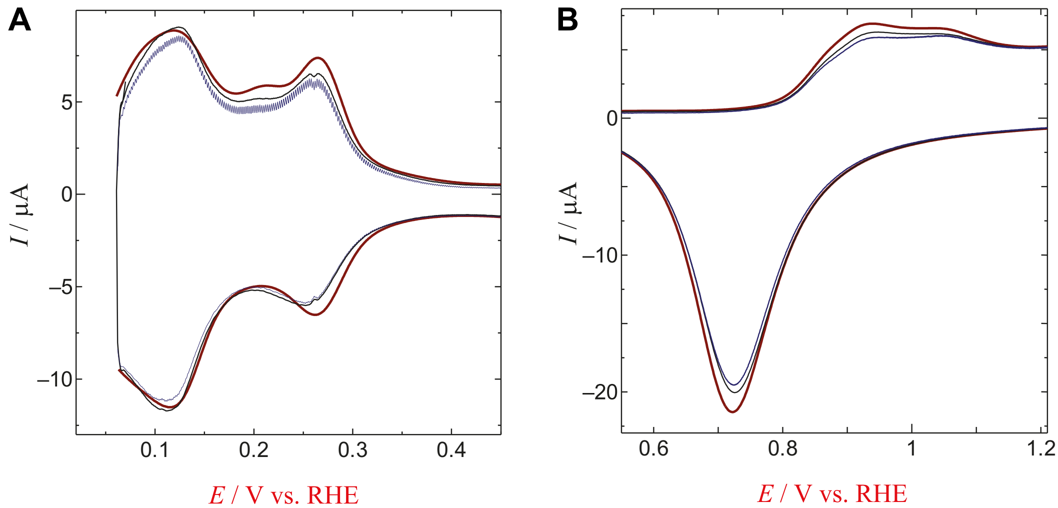

Fig. 2. CVs obtained at the poly-Pt electrode in N_2-saturated 0.1 M H_2SO_4 before poisoning (Brown) and after recovery experiments EX 1 (Blue) and EX 2 (Black). Scan rate: 100 mV s^{-1}. (For interpretation of the references to colour in this figure legend, the reader is referred to the web version of this article.)

in the presence of NH_4^+ ion corresponding to the oxidation of this cation. The current for the oxidation of NH_4^+ ion in $HClO_4$ solution was noticed to be higher compared to that in H_2SO_4 solution indicating an easier oxidation process in the former solution. The reduction peak of the Pt oxide layer at ~0.76 V vs. RHE in the cathodic potential scan decreased with increasing the concentration of NH_4^+ ion, and typically the decrease was found to be higher in H_2SO_4 (12%) than in $HClO_4$ (7%) in the presence of 100 ppm NH_4^+ ion. The effect of the NH_4^+ ion on the hydrogen adsorption was observed in the same manner as observed for the hydrogen desorption, although to a lower extent.

Several methods have been reported for the recovery of platinum catalysts in PEMFCs [20,23]. In situ voltammetric method is considered to be an efficient and convenient one for the removal of the adsorbed poisonous species. In the present case, two procedures for the recovery of the poisoned poly-Pt electrode in each electrolyte solution have been employed: by cycling the electrode potential (starting from the open circuit potential towards either cathodic (EX 1) or anodic (EX 2) direction of potential) between 0.06 and 1.56 V vs. RHE for 10 cycles at 100 mV s^{-1} in NH_4^+ ion-free H_2SO_4 or $HClO_4$ solutions. These methods of recovery are selected in this work as it has been reported that applying a constant potential, even as much as 1.6 V vs. NHE, does not completely recover a poisoned platinum electrode, and therefore potential cycling is essential for the complete recovery [34]. Fig. 2 shows the cyclic voltammograms (CVs) at the clean poly-Pt electrode (brown line) and at the recovered (by EX 1 (blue line) and EX 2 (black line)) poly-Pt electrodes in 0.1 M H_2SO_4 for the hydrogen adsorption-desorption (Fig. 2(A)) and the platinum oxide layer formation-reduction (Fig. 2(B)) regions. Poisoning of the clean Pt electrodes was performed by soaking the electrodes for 10 min in N_2-saturated 0.1 M H_2SO_4 containing 100 ppm NH_4^+ ion. Both of the recovery methods were found to be inadequate to recover the poisoned electrodes in H_2SO_4 solution. The charge of the hydrogen adsorption-desorption as well as the current for the formation of the Pt oxide layer and its reduction were found to be smaller compared to those at the clean poly-Pt electrodes. Fig. 3(A) and (B) show the CVs for the hydrogen adsorption-desorption and the platinum oxide layer formation-reduction regions, respectively, at the clean poly-Pt electrode (brown line) and at the recovered (by EX 1 (black line) and EX 2 (blue line)) poly-Pt electrodes in 0.1 M $HClO_4$ solution, in which poisoning of the electrodes was accomplished in

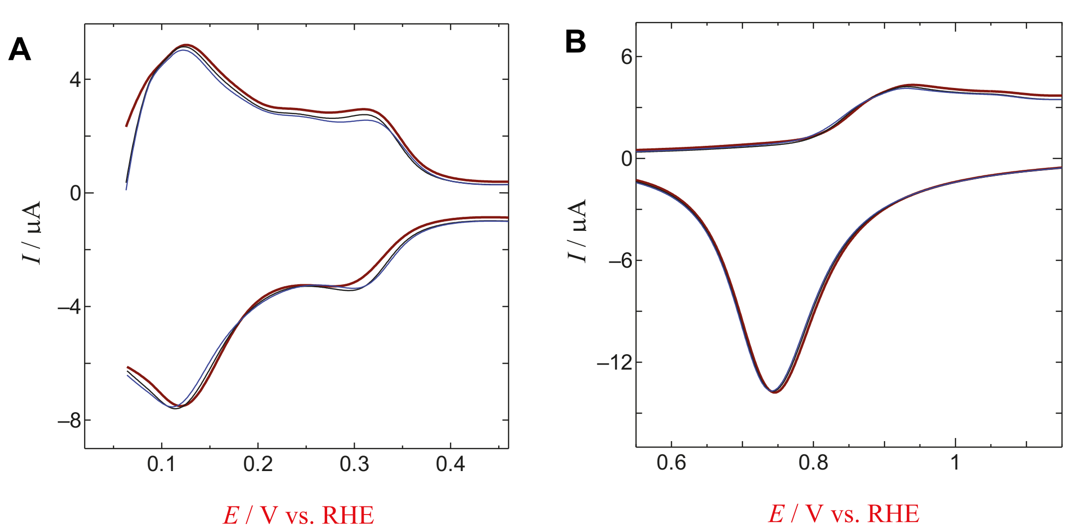

Fig. 3. CVs obtained at the poly-Pt electrode in N_2-saturated 0.1 M $HClO_4$ before poisoning (Brown) and after recovery experiments EX 1 (Black) and EX 2 (Blue). Scan rate: 100 mV s^{-1}. (For interpretation of the references to colour in this figure legend, the reader is referred to the web version of this article.)

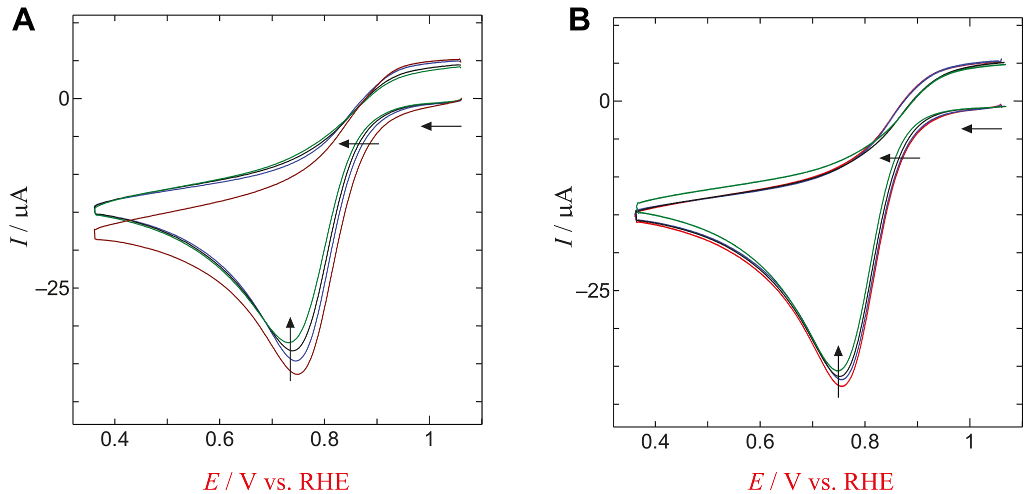

Fig. 4. (A) CVs obtained at the poly-Pt electrode in O_2-saturated 0.1 M H_2SO_4 solution (Brown) containing 1 (Blue), 10 (Black) and 100 (Green) ppm NH_4^+ ion. (B) CVs obtained at the poly-Pt electrode (Red) and recovered poly-Pt electrodes (after each measurement of ORR in the presence of 1 (Blue), 10 (Black) and 100 (Green) ppm NH_4^+ ion) in O_2-saturated NH_4^+ ion-free 0.1 M H_2SO_4 solution. Scan rate: 100 mV s^{-1}. (For interpretation of the references to colour in this figure legend, the reader is referred to the web version of this article.)

0.1 M $HClO_4$ according to the same procedure as used for the case in H_2SO_4. Interestingly, a complete recovery was observed in the both regions in 0.1 M $HClO_4$, in terms of total charge. A more significant oxidation of the adsorbed NH_4^+ ion in $HClO_4$ than in H_2SO_4 (Fig. 1) may account for such an improved recovery. The recovery procedures in the both electrolytic solutions were found to be reproducible. The peak currents and the peak potentials in the hydrogen adsorption–desorption regions as well as in the Pt oxide layer formation and its reduction regions did not change for a non-poisoned electrode after the same recovery treatment in ammonium free H_2SO_4 and $HClO_4$ solutions.

Fig. 4(A) shows the ORR at the poly-Pt electrode in 0.1 M H_2SO_4 solution in the absence and presence of various amounts of NH_4^+ ion. The onset potential and the peak current of the ORR at this electrode in the absence of any NH_4^+ ion (Fig. 4(A): brown curve) were found to shift towards the negative direction of potential and decrease, respectively, with increasing the concentration of NH_4^+ ion. As much as 30 mV negative shift of the onset potential and 12% decrease in the peak current were recognized in the presence of 100 ppm NH_4^+ ion. In order to verify the efficiency of the recovery method, recovery experiment was performed after each measurement of the ORR in the presence of various concentrations of NH_4^+ ion and the ORR was performed at these recovered electrodes in O_2-saturated NH_4^+ ion-free 0.1 M H_2SO_4 solution (Fig. 4(B)). A negative shift of the onset potential as well as a decrease in the peak current for the ORR at the each recovered electrode account for the weak efficiency of the recovery method in H_2SO_4. On the other hand, the ORR at the poly-Pt electrode in 0.1 M $HClO_4$ solution experienced a milder poisoning effect from NH_4^+ ion compared to that in 0.1 M H_2SO_4 solution. Fig. 5(A) shows the effect of various concentrations of NH_4^+ ion on the ORR at the poly-Pt electrode in 0.1 M $HClO_4$. In the presence of 100 ppm NH_4^+ ion, a negative shift of the onset potential (16 mV) as well as a decrease in the ORR current (5%) were noticed, which are lower in value compared to those observed in 0.1 M H_2SO_4 in the presence of the same amount of NH_4^+ ion. Fig. 5(B) shows the CVs obtained at the clean poly-Pt electrode (Red) and recovered poly-Pt electrodes (after each measurement of ORR in the presence of 1 (Blue), 10 (Black) and 100 (Green) ppm NH_4^+ ion) in O_2-saturated NH_4^+ ion-free 0.1 M $HClO_4$ solution. Interestingly, both the onset potential and the peak current for the

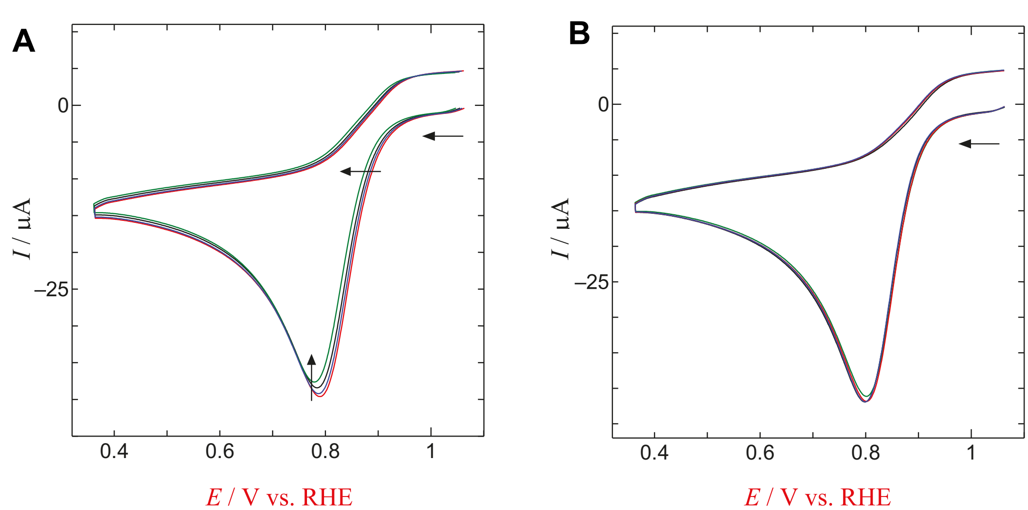

Fig. 5. (A) CVs obtained at the poly-Pt electrode in O_2-saturated 0.1 M $HClO_4$ solution (Red) containing 1 (Blue), 10 (Black) and 100 (Green) ppm NH_4^+ ion. (B) CVs obtained at the poly-Pt electrode (Red) and recovered poly-Pt electrodes (after each measurement of ORR in the presence of 1 (Blue), 10 (Black) and 100 (Green) ppm NH_4^+) in O_2-saturated NH_4^+ ion-free 0.1 M $HClO_4$ solution. Scan rate: 100 mV s^{-1}. (For interpretation of the references to colour in this figure legend, the reader is referred to the web version of this article.)

ORR obtained at any of the recovered electrodes were found to be almost the same as those at the clean poly-Pt electrode, supporting an excellent recovery in the $HClO_4$ solution.

The hydrodynamic voltammograms for the ORR were obtained at the poly-Pt electrode in O_2-saturated 0.1 M H_2SO_4 (Fig. 6(A)) and 0.1 M $HClO_4$ (Fig. 6(B)) solutions containing 100 ppm NH_4^+ ion at electrode rotation rates in the range of 400–2000 rpm and at a potential scan rate of 10 mV s^{-1}. Recovery of the electrode was carried out after each run. The dotted curves in each figure represent the background current obtained at rotation rate of 2000 rpm in the presence of 100 ppm NH_4^+ ion. The background current was subtracted from the total current for obtaining the net current for the ORR. The limiting current (I_L) for the ORR at the rotating disk electrode (RDE) can be presented by Eq. (1) known as Levich equation [35–37]:

$$I_L = 0.62nFAC_bD_0^{2/3}\nu^{-1/6}\omega^{1/2} \quad (1)$$

where n is the number of electrons involved in the reduction of O_2, F is the Faraday constant (96,485 C mol^{-1}), A is the geometric surface area of the RDE, C_b is the bulk concentration of O_2 (1.1×10^{-3} mol dm^{-3}), D_0 is the diffusion coefficient of O_2 (1.93×10^{-5} cm^2 s^{-1}), ν is the kinematic viscosity of the solution (ca. 0.01 cm^2 s^{-1}) [38] and ω is the angular rotation rate of the electrode expressed as radian per second ($\omega = 2\pi f/60$, where f is the rotation in rpm). Thus the above equation gives a linear dependence of I_L on $\omega^{1/2}$ with a zero intercept and a slope proportional to the apparent number of electrons exchanged per O_2 molecule in the overall cathodic reaction. The limiting current densities (J_L) were obtained at 0.26 V vs. RHE from the hydrodynamic voltammograms shown in Fig. 6(A) and (B) and plotted as a function of $\omega^{1/2}$ (Fig. 6(C) and (D): blue lines, respectively). In both cases, the experimental values nicely fall on a straight line passing through the origin, suggesting that the reaction is controlled by the mass transfer of O_2 to the electrode surface. The slopes of the experimental lines were obtained as 0.34 mA cm^{-2} (rad $s^{-1})^{-1/2}$ and 0.43 mA cm^{-2} (rad $s^{-1})^{-1/2}$ in H_2SO_4 and $HClO_4$ solutions, respectively. Similar experiments have also been carried out in the absence of any NH_4^+ ion in these two electrolytic solutions (figure not shown here) and the limiting current densities (J_L) were obtained at 0.26 V vs. RHE from the hydrodynamic voltammograms and plotted as a function of $\omega^{1/2}$ (Fig. 6(C) and (D): red lines). The values of J_L were also calculated based on Eq. (1) using the values of n equal to 4 and other parameters as given above and plotted as a function of $\omega^{1/2}$(Fig. 6(C) and (D): black dashed lines). The slopes of the experimental lines in the absence of NH_4^+ ion were obtained as 0.43 mA cm^{-2} (rad $s^{-1})^{-1/2}$

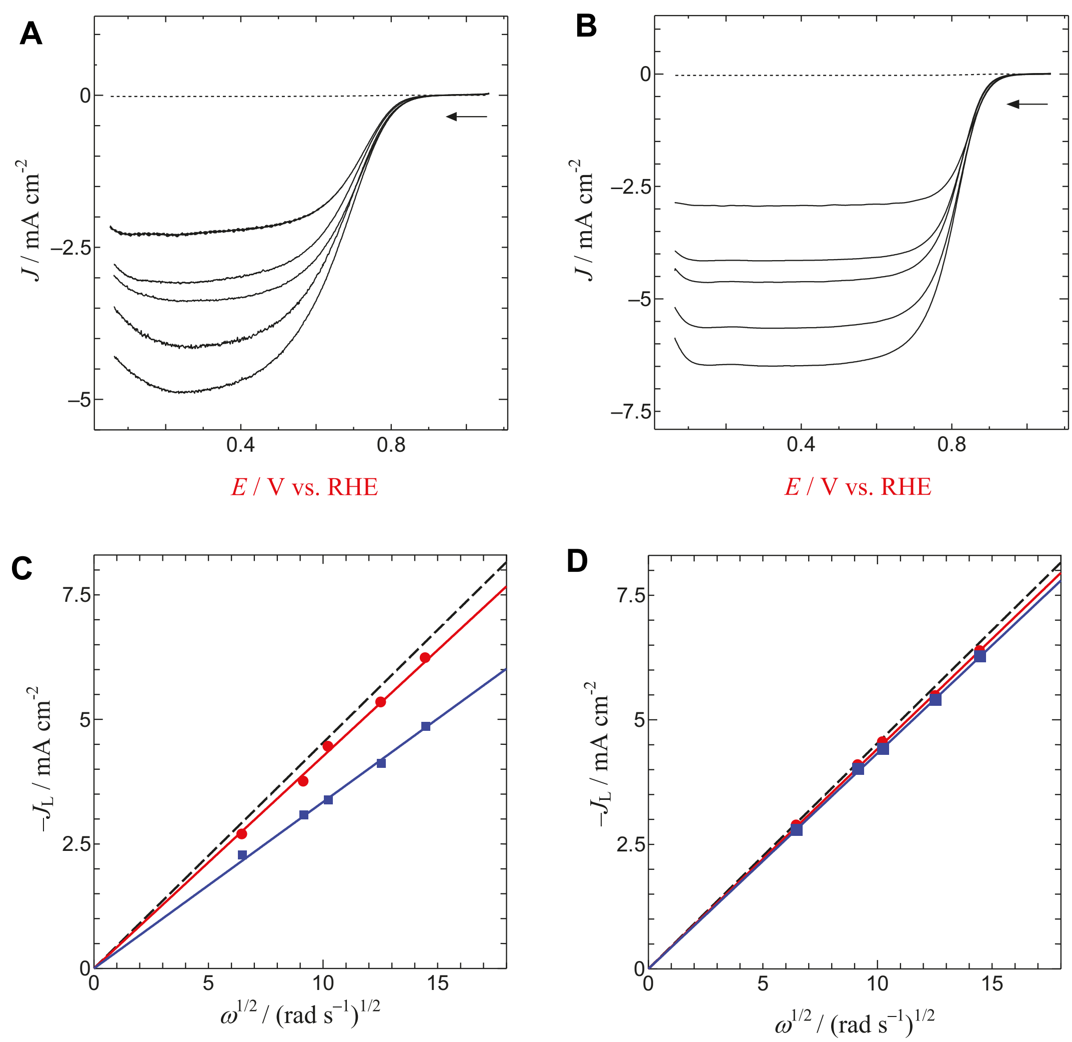

Fig. 6. Steady-state voltammograms obtained for the ORR at the Pt RDE in O_2-saturated 0.1 M H_2SO_4 (A) and 0.1 M $HClO_4$ (B) solutions containing 100 ppm NH_4^+ ion. Rotation rate: 400, 800, 1000, 1500 and 2000 rpm. Scan rate: 10 mV s^{-1}. Recovery was performed after each measurement. Levich plots are shown for the ORR at the Pt RDE in O_2-saturated 0.1 M H_2SO_4 (C) and 0.1 M $HClO_4$ (D) solutions containing 0 (Red) and 100 (Blue) ppm NH_4^+ ion. The dashed lines correspond to the theoretically predicted ones for four-electron reduction of O_2. (For interpretation of the references to colour in this figure legend, the reader is referred to the web version of this article.)

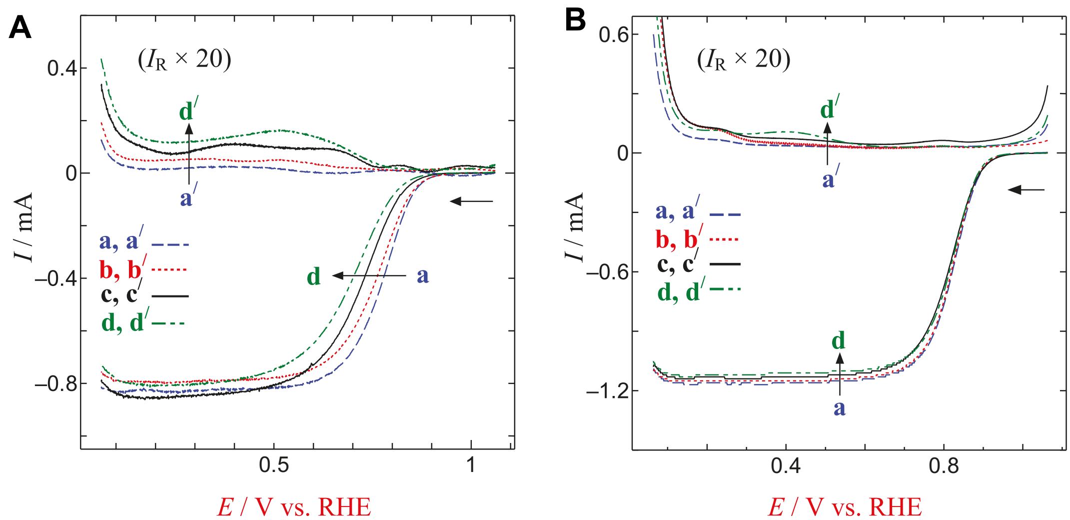

Fig. 7. (A) Steady-state voltammograms obtained for the ORR at Pt-disk electrode (a–d) and for the oxidation of H_2O_2 at Pt-ring electrode (a′-d′ in O_2-saturated 0.1 M H_2SO_4 solution in the absence (a, a') and presence of 1 (b, b′), 10 (c, c′) and 100 (d, d′) ppm NH_4^+ ion. (B) Same notations as 'A' in 0.1 M $HClO_4$ solution. Scan rate: 10 mV s^{-1}, rotation rate: 800 rpm, the Pt ring was potentiostated at 1.26 V vs. RHE and the ring currents are shown as 20 times of their original magnitude. Recovery was performed after each measurement.

and 0.44 mA cm^{-2} (rad $s^{-1})^{-1/2}$ in H_2SO_4 and $HClO_4$ solutions, respectively, which are consistent with the slope of the theoretical line for $n = 4$ (0.45 mA cm^{-2} (rad $s^{-1})^{-1/2}$), suggesting that the ORR at the poly-Pt electrode proceeds through an exclusive four-electron pathway in the absence of NH_4^+ ion. In the presence of 100 ppm NH_4^+ ion, the ORR at the poly-Pt electrode in 0.1 M $HClO_4$ actually follows the four-electron pathway, while a smaller slope obtained in 0.1 M H_2SO_4 suggests a decrease in the active surface area and/or a contribution of a two-electron reduction of O_2 in the ORR.

In order to investigate the reason behind the significant decrease in the ORR current, i.e., whether it originates from decrease in the active surface area or change in the mechanism of the ORR, the rotating ring-disk electrode voltammetry was conducted in H_2SO_4 and $HClO_4$ solutions in the presence of various amounts of NH_4^+ ion (1, 10 and 100 ppm). The disk currents (I_D) of the ORR are shown as the negative current while the ring currents (I_R) for the oxidation of H_2O_2 as the positive current. The ring currents are shown as 20 times of their original magnitude. The RRDE voltammograms in the NH_4^+ ion-free acids ((a, a') of Fig. 7(A) and (B)) show significantly small ring currents indicating the exclusive four-electron reduction of O_2 to H_2O in the both electrolytic solutions. Upon addition of NH_4^+ ion, the onset potential of the ORR was found to shift towards the negative direction of potential and the ORR current also decreased in H_2SO_4 (Fig. 7(A)). In this case, the ring current was also noticed to be higher. The negative shifting of the onset potential, decrease in the ORR current and increase in the ring current became remarkable with increasing the concentration of NH_4^+ ion. In the presence of NH_4^+ ion, the increase in the ring current indicates the significant contribution of the two-electron pathway of ORR (formation of H_2O_2) due to the adsorption of the nitrogen species which might partially change the adsorption pattern of the molecular oxygen from a parallel mode to an end-top mode. Such a change in the ORR mechanism occurs due to the decrease in the number of adjacent adsorption sites necessary for the breaking of the O–O bond [17]. In $HClO_4$ solution, no change in the onset potential of the ORR was recognized in the presence of NH_4^+ ion of 1, 10 and 100 ppm and only a slight decrease in the ORR current and increase in the ring current were noticed with increasing the concentration of NH_4^+ ion, indicating the almost exclusive four-electron pathway of the ORR even in the presence of 100 ppm NH_4^+ ion.

The RRDE voltammograms were also recorded at the pre-oxidized and pre-reduced electrodes in the absence and presence of 1, 10 and 100 ppm NH_4^+ ion in 0.1 M H_2SO_4 and 0.1 M $HClO_4$ solutions. Potential was scanned towards the positive direction of potential starting from 0.06 V vs. RHE at the pre-reduced electrode in contrast to that at the untreated and pre-oxidized electrodes. Fig. 8(A) and (B) show the typical results obtained for the ORR at the clean (a, a′, b, b′), pre-oxidized (c, c′) and pre-reduced (d, d′) Pt RRDE electrodes in the absence (a, a′) and presence (b–d, b′–d′) of 100 ppm NH_4^+ ion in 0.1 M H_2SO_4 (Fig. 8(A)) and 0.1 M $HClO_4$ (Fig. 8(B)) solutions. In H_2SO_4 solution, the onset potential of the ORR shifted towards the negative direction of potential, the ORR current decreased and the ring current increased at all the electrodes in the presence of 100 ppm NH_4^+ ion. At this concentration of NH_4^+ ion, the onset potentials shifted negatively by 40, 45 and 100 mV at the untreated, pre-oxidized and pre-reduced electrodes, respectively, compared to those at the respective electrodes in NH_4^+ ion-free 0.1 M $HClO_4$. The reaction rate of the ORR has been reported to largely depend on the pre-treatment potential [39]. At the pre-oxidized electrode, the ORR was affected by the formation of platinum oxide layer [40] and the deleterious effect at the pre-reduced electrode may originate from the hydrogen or anion adsorption. Far better results were obtained in 0.1 M $HClO_4$ solution for the ORR at all the electrodes in the presence of 100 ppm NH_4^+ ion. The onset potentials of the ORR in the presence of NH_4^+ ion at the untreated, pre-oxidized and pre-reduced electrodes shifted negatively only by 10, 15 and 25 mV, respectively, compared with those obtained at the respective electrodes in NH_4^+ ion-free 0.1 M $HClO_4$.

The percentage of the electrogenerated hydrogen peroxide ($X_{H_2O_2}$) and the number of electron transferred (n) during the ORR at all three electrodes in the absence and presence of 1, 10 and 100 ppm NH_4^+ ion were calculated using Eqs. (2) and (3):

$$n = \frac{4I_R}{I_D + I_R/N} \tag{2}$$

$$X_{H_2O_2} = \frac{200 I_R/N}{I_D + I_R/N} \tag{3}$$

where, I_D and I_R are the disk and ring currents, respectively and N is the collection efficiency (0.41). Fig. 8(C) and (D) show the typical

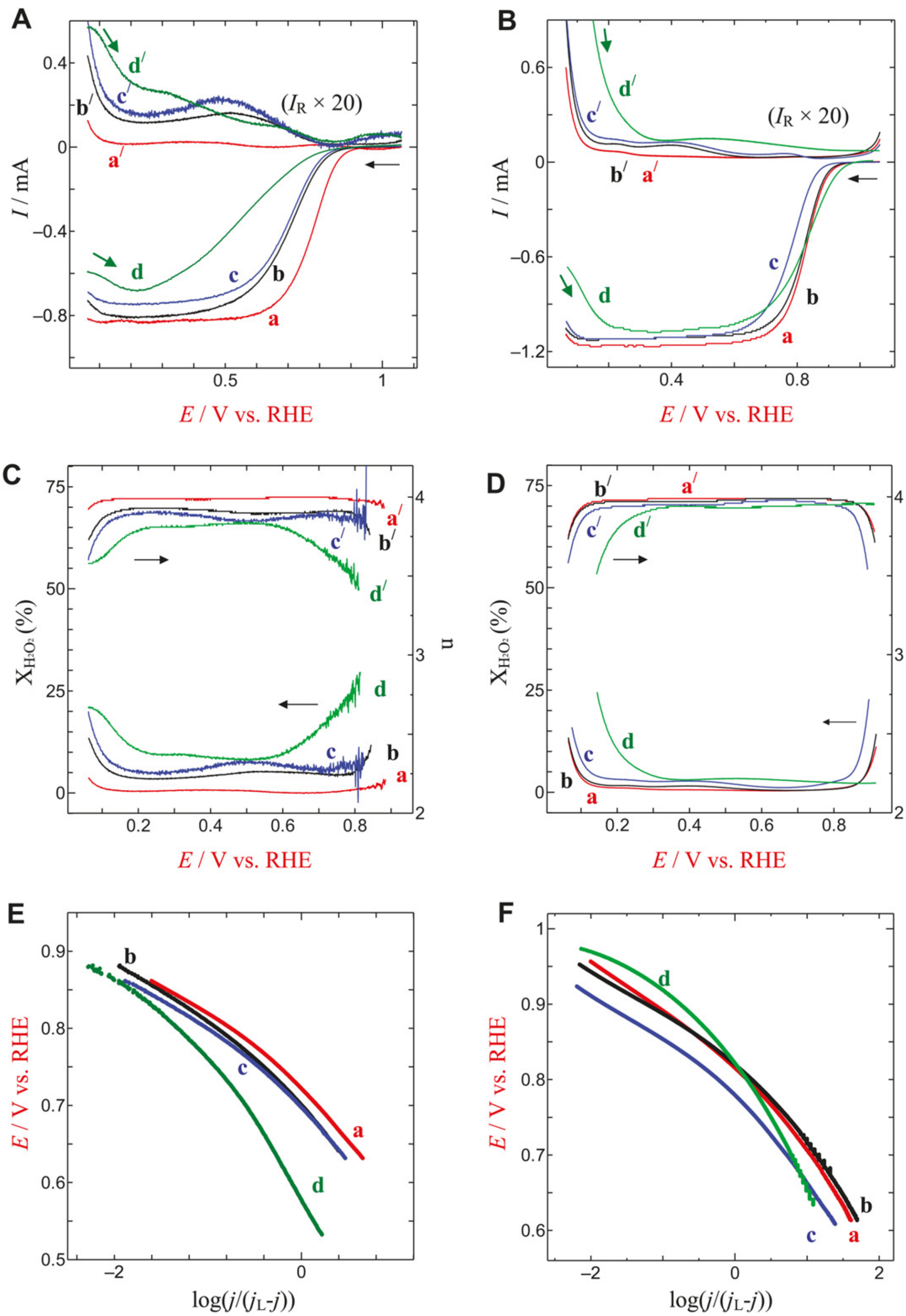

Fig. 8. (A) Steady-state voltammograms obtained for the ORR at Pt-disk electrode (a–d) and for the oxidation of H_2O_2 at Pt-ring electrode (a'–d') in O_2-saturated 0.1 M H_2SO_4 solution in the absence (a, a') and presence (b, b') of 100 ppm NH_4^+ ion. (c, c') and (d, d') are the same notations as (b, b') but the potential scanning was performed towards the cathodic and anodic direction of potential for the pre-oxidized and pre-reduced electrodes, respectively. Scan rate: 10 mV s^{-1}, rotation rate: 800 rpm, the Pt ring was potentiostated at 1.26 V vs. RHE and the ring currents are shown as 20 times of their original magnitude. (C) Variation of the number of transferred electrons (n) during the ORR (a'–d') and the percentage of the electro-generated H_2O_2 ($X_{H_2O_2}$) (a–d) without pre-treatment (a, a', b, b'), and with anodic pre-treatment (c, c') and cathodic pre-treatment (d, d') of the Pt-disk electrode in the absence (a, a') and presence (b–d, b'–d') of 100 ppm NH_4^+ ion. (E) Mass-transfer corrected Tafel plots for the ORR in untreated (a, b), anodically pre-treated (c) and cathodically pre-treated (d) Pt-disk electrodes in the absence (a) and presence (b, c, d) of 100 ppm NH_4^+ ion. (B), (D) and (F) represent the same notations as 'A', 'B' and 'C', respectively, in 0.1 M $HClO_4$ solution.

potential dependence of $X_{H_2O_2}$ and n at the untreated (a, b and a', b'), pre-oxidized (c and c') and pre-reduced (d and d') electrodes in the absence (a and a') and presence of (b–d and b'–d') 100 ppm NH_4^+ ion in 0.1 M H_2SO_4 (Fig. 8(C)) and 0.1 M $HClO_4$ (Fig. 8(D)) solutions. In H_2SO_4 solution, in the presence of 100 ppm NH_4^+ ion, 4, 6 and 10% H_2O_2 were generated and the n value was reduced to

Table 1
Tafel slopes obtained at (b1) low and (b2) high current densities at the various Pt electrodes.

$[NH_4^+]$/ppm	Tafel slope/mV decade^{-1}											
	Untreated electrode[a]				Pre-oxidized electrode[b]				Pre-reduced electrode[c]			
	H_2SO_4		$HClO_4$		H_2SO_4		$HClO_4$		H_2SO_4		$HClO_4$	
	b1	b2	b1	b2	b1	b2	b1	b2	b1	b2	b1	b2
0	71	122	62	123	76	130	59	120	80	158	66	156
1	78	130	65	122	80	134	58	122	84	165	67	158
10	80	138	68	125	83	130	63	124	89	170	64	155
100	81	134	64	121	79	132	62	123	98	198	71	162

[a] The potential was scanned in the cathodic direction without pre-treatment.
[b] The Pt-disk electrode of the RRDE was potentiostated at 1.06 V vs. RHE for 10 min before scanning the potential in the cathodic direction.
[c] The Pt-disk electrode of the RRDE was potentiostated at 0.06 V vs. RHE for 10 min before scanning the potential in the anodic direction.

3.90, 3.86 and 3.80 at 0.1 V at the untreated, pre-oxidized and pre-reduced electrodes, respectively, confirming the existence of the two-electron pathway of ORR along with the four-electron one. On the other hand, in $HClO_4$ solution, the values for the $X_{H_2O_2}$ and n at the untreated, pre-oxidized and pre-reduced electrodes were calculated as 1.5% and 3.97, 2.5% and 3.96 and 3.0% and 3.95, respectively, at 0.1 V in the presence of 100 ppm NH_4^+ ion, indicating a minor effect of the pre-treatment of electrode on the four-electron pathway of the ORR in the $HClO_4$ solution.

Mass transfer corrected Tafel plots of the ORR in the 0.1 M H_2SO_4 and 0.1 M $HClO_4$ solutions were drawn for the untreated, pre-oxidized and pre-reduced electrodes in the absence and presence of 1, 10 and 100 ppm NH_4^+ ion and the Tafel slopes are presented in Table 1. Fig. 8(E) and (F) show the typical Tafel plots obtained for the ORR at the untreated (a, b), pre-oxidized (c) and pre-reduced (d) electrodes in the absence (a) and presence (b–d) of 100 ppm NH_4^+ ion in 0.1 M H_2SO_4 (Fig. 8(E)) and 0.1 M $HClO_4$ (Fig. 8(F)) solutions. From Fig. 8(E) and Table 1 we can see that, at the untreated electrode, the Tafel slope at low current density in pure H_2SO_4 solution is higher than that expected according to the Damjanovic mechanism [39], −71 vs.−60 mV/decade, and the Tafel slope at high current density is in line with the prediction, i.e., −122 vs.−120 mV/decade. It should be noted that the determination of the Tafel slope at low current density is difficult as the plot is curved actually. In the pure H_2SO_4 solution, the Tafel slopes at low and high current densities increased at the pre-oxidized and pre-reduced electrodes compared to those at the untreated electrode revealing the negative effect of the pre-treatment procedure on the ORR. The slopes at these three electrodes were further increased with increasing the concentration of NH_4^+ ion and attained−98 and−198 mV/decade for the low and high current densities, respectively, at the pre-reduced electrode in the presence of 100 ppm NH_4^+ ion, demonstrating the deleterious effect of the NH_4^+ ion on the ORR. On the other hand, the Tafel slopes at the low and high current densities at the untreated and pre-oxidized electrodes in the pure $HClO_4$ solution were found to be in line with the Damjanovic prediction confirming no effect of NH_4^+ ion on the ORR in this electrolytic solution. However, at the pre-reduced electrode, a higher Tafel slope (−156 mV/decade) was obtained at the high current density region in the pure $HClO_4$ solution. Zecevic et al. also observed a higher Tafel slope (−135 mV/decade) than expected at the high current density region in pure $HClO_4$ solution [41]. The Tafel slopes at this electrode at the low and high current densities were found to increase only a little in the presence of 100 ppm NH_4^+ ion. The differences in the Tafel slopes at the pre-reduced electrode in 0.1 M $HClO_4$ solution in the absence and presence of various amounts of NH_4^+ ion can be considered insignificant by taking the uncertainty in the Tafel slope fitting procedure into account.

4. Conclusions

The low concentration ammonium ion poisoning of the poly-Pt electrode was investigated in two different electrolytic solutions, i.e., H_2SO_4 and $HClO_4$. A significant effect of ammonium ion on the catalytic activity towards ORR at the poly-Pt electrode was realized in H_2SO_4 solution in contrast to the results of the Okada et al. who reported a decrease in the ORR current due to an interaction between the NH_4^+ ion and the ionomer on the Nafion® film-covered Pt electrode [26]. They reported even smaller effect of NH_4^+ ion [26] than that of Na^+ and K^+ [42] on the ORR. However, a comparative investigation of the ORR at the Nafion®-coated Pt electrode in the H_2SO_4 and $HClO_4$ solutions containing NH_4^+ ion may disclose such interaction. A complete recovery of the poisoned electrode was achieved in NH_4^+ ion-free $HClO_4$ solution by cycling the potential 10 times between the onset potentials of the hydrogen and oxygen evolution, while this method was not effective enough to recover the poisoned electrode in H_2SO_4 solution. The experimentally determined Levich slope for the ORR at the poly-Pt electrode in $HClO_4$ solution containing ammonium ion was in good agreement with the theoretically predicted slope for $n = 4$, suggesting the four-electron pathway of the ORR. On the other hand, the Levich slope was noticed to decrease in H_2SO_4 solution containing NH_4^+ ion revealing the significant contribution of the two-electron pathway of O_2 to H_2O_2 in the ORR. The Tafel slope was found to increase with increasing the concentration of NH_4^+ ion in H_2SO_4 at all the electrodes confirming the deleterious effect of the NH_4^+ ion on the ORR. However, the Tafel slopes at all the electrodes in $HClO_4$ solution containing various amounts of NH_4^+ ion were almost comparable to that in the pure $HClO_4$ solution suggesting a minute effect of the NH_4^+ ion on the ORR in this electrolytic solution.

Acknowledgements

This work was financially supported by a Grant-in-Aid for Scientific Research (A) (No. 19206079) to T.O. from the Ministry of Education, Culture, Sports, Science and Technology (MEXT), Japan and also by the New Energy and Industrial Technology Development Organization (NEDO), Japan.

References

[1] O. Antoine, Y. Bultel, R. Durand, J. Electroanal. Chem. 499 (2001) 85–94.
[2] S. Strbac, R.R. Adzic, Electrochim. Acta 41 (1996) 2903–2908.
[3] M.S. El-Deab, T. Ohsaka, J. Electrochem. Soc. 155 (2008) D14–D21.
[4] T.J. Schmidt, U.A. Paulus, H.A. Gasteiger, R.J. Behm, J. Electroanal. Chem. 508 (2001) 41–47.
[5] S. Guerin, G.S. Attard, Electrochem. Commun. 3 (2001) 544–548.
[6] A. Kuzume, E. Herrero, J.M. Feliu, J. Electroanal. Chem. 599 (2007) 333–343.
[7] K. Miyatake, T. Omata, D.A. Tryk, H. Uchida, M. Watanabe, J. Phys. Chem. C 113 (2009) 7772–7778.
[8] O.A. Petrii, J. Solid State Electrochem. 5 (2008) 609–642.
[9] R. Halseid, M. Heinen, Z. Jusys, R.J. Behm, J. Power Sourc. 176 (2008) 435–443.
[10] R. Mohtadi, W.-K. Lee, S. Cowan, J.W. Van Zee, M. Murthy, Electrochem. Solid-State Lett. 6 (2003) A272–A274.
[11] J.M. Moore, P.L. Adcock, J.B. Lakeman, G.O. Mepsted, J. Power Sourc. 85 (2000) 254–260.
[12] R. Mohtadi, W.-K. Lee, J.W. Van Zee, J. Power Sourc. 138 (2004) 216–225.

[13] F. Garzon, F.A. Uribe, T. Rockward, I.G. Urdampilleta, E.L. Brosha, ECS Trans. 3 (2006) 695–703.
[14] Y. Yoshimura, M. Toba, T. Matsui, M. Harada, Y. Ichihashi, K.K. Bando, H. Yasuda, H. Ishihara, Y. Morita, T. Kameoka, Appl. Catal. A: Gen. 322 (2007) 152–171.
[15] J. Fu, M. Hou, C. Du, Z. Shao, B. Yi, J. Power Sourc. 187 (2009) 32–38.
[16] J.H. Wang, M. Liu, J. Power Sourc. 176 (2008) 23–30.
[17] S. Imabayashi, Y. Kondo, R. Komori, A. Kawano, T. Ohsaka, ECS Trans. 16 (2008) 925–930.
[18] Y. Nagahara, S. Sugawara, K. Shinohara, J. Power Sourc. 182 (2008) 422–428.
[19] Y. Zhai, G. Bender, S. Dorn, R. Rocheleau, J. Electrochem. Soc. 157 (2010) B20–B26.
[20] Y. Garsany, O.A. Baturina, K.E. Swider-Lyons, J. Electrochem. Soc. 154 (2007) B670–B675.
[21] D. Pillay, M.D. Johannes, Y. Garsany, K.E. Swider-Lyons, J. Phys. Chem. C 114 (2010) 7822–7830.
[22] B.D. Gould, O.A. Baturina, K.E. Swider-Lyons, J. Power Sourc. 188 (2009) 89–95.
[23] Y. Garsany, O.A. Baturina, K.E. Swider-Lyons, J. Electrochem. Soc. 156 (2009) B848–B855.
[24] O.A. Baturina, K.E. Swider-Lyons, J. Electrochem. Soc. 156 (2009) B1423–B1430.
[25] R. Halseid, T. Bystron, R. Tunold, Electrochim. Acta 51 (2006) 2737–2742.
[26] T. Okada, H. Satou, M. Yuasa, Langmuir 19 (2003) 2325–2332.
[27] F.A. Uribe, S. Gottesfeld, T.A. Zawodzinski Jr., J. Electrochem. Soc. 149 (2002) A293–A296.
[28] H.J. Soto, W.-K. Lee, J.W. Van Zee, M. Murthy, Electrochem. Solid State Lett. 6 (2003) A133–A135.
[29] S.T. Szymanski, G.A. Gruver, M. Katz, H.R. Kunz, J. Electrochem. Soc. 127 (1980) 1440–1444.
[30] S. Thomas, Y.-E. Sung, H.S. Kim, A. Wieckowski, J. Phys. Chem. 100 (1996) 11726–11735.
[31] A. Kolics, A. Wieckowski, J. Phys. Chem. B 105 (2001) 2588–2595.
[32] G. Kokkinidis, D. Jannakoudakis, J. Electroanal. Chem. Interfacial Electrochem. 162 (1984) 163–173.
[33] C.F. Zinola, A.M. Castro Luna, W.E. Triaca, A.J. Arvia, J. Appl. Electrochem. 24 (1994) 531–541.
[34] T. Loucka, J. Electroanal. Chem. 31 (1971) 319–332.
[35] C.-C. Chang, T.-C. Wen, H.-J. Tien, Electrochim. Acta 42 (1997) 557–565.
[36] A.J. Bard, L.R. Faulkner, Electrochemical Methods: Fundamental and Applications (Chaps. 3 and 9), John Wiley and Sons, Inc., New York, 2001 (and the refs in therein).
[37] Md.R. Miah, T. Ohsaka, J. Electrochem. Soc. 154 (2007) F186–F190.
[38] M. Tsushima, K. Tokuda, T. Ohsaka, Anal. Chem. 66 (1994) 4551–4556.
[39] A. Damjanovic, O.J. Murphy, S. Srinivasan, B.E. Conway (Eds.), Electrochemistry in transition, from the 20th to the 21st century, Plenum Press, New York, 1992, p. 107.
[40] T.D. Jarvi, in: T.W. Patterson Jr., N.E. Cipollini, J.B. Hertzberg, M.L. Perry (Eds.), Proceedings of the 203rd Meeting of The Electrochemical Society, The Electrochemical Society, Inc., 65 South Main Street, Pennington, NJ, USA, 2003 (Meeting abstracts).
[41] S.K. Zecevic, J.S. Wainright, M.H. Litt, S.L. Gojkovic, R.F. Savinell, J. Electrochem. Soc. 144 (1997) 2973–2982.
[42] T. Okada, J. Dale, Y. Ayato, O.A. Asbjornsen, M. Yuasa, I. Sekine, Langmuir 15 (1999) 8490–8496.